ELSEVIER

Journal of Crystal Growth 175/176 (1997) 888–893

JOURNAL OF CRYSTAL GROWTH

Stranski–Krastanov growth of InSb, GaSb, and AlSb on GaAs: structure of the wetting layers

B.R. Bennett[1], B.V. Shanabrook, P.M. Thibado[2], L.J. Whitman, R. Magno

Naval Research Laboratory, Washington, DC 20375-5347, USA

Abstract

Thin layers of InSb, GaSb and AlSb were grown on GaAs(0 0 1) by molecular beam epitaxy and characterized in situ with scanning tunneling microscopy. All three materials exhibit a Stranski–Krastanov growth mode. Distinct wetting layers and self-assembled quantum dots are present after deposition of one to four monolayers of (In,Ga,Al)Sb. The wetting layers consist of anisotropic, ribbon-like structures oriented along the [$\bar{1}$ 1 0] direction, with characteristic separations of 40–50 Å. The initial GaAs surface reconstruction affects both the wetting layer structure and the quantum dot density.

1. Introduction

The Stranski–Krastanov (SK) growth mode in strained-layer heteroepitaxy has been recognized for decades [1–3]. In this mode, the deposited layer initially grows as a two-dimensional (2D) wetting layer for at least one monolayer. Then, three-dimensional (3D) islands form on the wetting layer. Recently, there has been considerable interest in using SK growth to deposit coherent islands, known as self-assembled quantum dots (QDs). These QDs have been reported in semiconductor systems including InAs/GaAs, InP/InGaP, and GaSb/GaAs [4–8]. Although QDs with size uniformities on the order of 10% are routinely achieved, many potential applications such as solid-state lasers require more uniform ensembles of QDs. Theoretical work suggests that the uniformity of QDs is related to the structure of the wetting layer, [9–11] but few experimental studies have been reported [12–15]. In this work, we apply in-situ scanning tunneling microscopy (STM) to investigate the structure of wetting layers of GaSb, AlSb and InSb on GaAs (mismatches of 7.8%, 8.5% and 14.6%, respectively) grown by molecular beam epitaxy (MBE). In all three cases, we observe wetting layers composed of 2D islands with anisotropic ribbon-like structure and characteristic inter-island separations of 40–50 Å.

2. Experimental procedure

Experiments were carried out in an interconnected multi-chamber ultra-high vacuum (UHV)

[1] E-mail: bennett@bloch.nrl.navy.mil.

[2] Present address: Department of Physics, University of Arkansas, Fayetteville, Arkansas 72701, USA.

PII S0022-0248(96)00917-7

facility that includes a III–V solid-source MBE and a surface analysis chamber with STM. All growths were performed on n^+ GaAs, oriented to within 0.1° of (0 0 1). Growth temperatures were determined by GaAs band-edge transmission thermometry [16]. First, a GaAs buffer layer 0.5–1.0 μm thick was grown at 580°C (with interrupts) at a growth rate of 1.0 monolayer (ML)/s with the growth monitored by reflection high-energy electron diffraction (RHEED). During the GaAs buffer growth, the RHEED pattern was a streaky (2×4) reconstruction. Before the growth of each antimonide layer, a 3–5 min growth interrupt was performed at 580°C under an As_4 flux, resulting in the appearance of sharp diffraction spots along each streak. A well-ordered (2×4) or $c(4\times4)$ reconstruction was then prepared by alternately lowering the substrate temperature and As flux until the point at which the As valve could be closed without degradation of the RHEED pattern. This technique produces GaAs surfaces with ~ 5000 Å-wide terraces separated by monolayer-height (3 Å) steps [17]. The antimonide layer was grown by migration-enhanced epitaxy with a cation deposition rate of 0.10 ML/s and a V : III flux ratio of approximately 2 : 1. For example, to grow 1.5 ML of InSb, the shutter sequence was: 5 s In, 20 s Sb, 5 s In, 20 s Sb, 5 s In, 20 s Sb. After deposition of the III-Sb monolayers, the sample was held at the growth temperature under an Sb_4 flux for 120 s before cooling. Finally, the sample was transferred under UHV to the STM chamber and imaged at room temperature. All STM images displayed here were acquired in constant-current mode with currents between 0.1 and 1.0 nA and sample biases ranging from −2.0 to −3.2 V. The images are displayed in gray-scale without corrections for thermal drift.

3. Results

Well-ordered surfaces are observed for GaAs(0 0 1)-(2×4) and -$c(4\times4)$, in contrast to the disordered surface revealed by both RHEED and STM after the deposition of 1–4 ML of GaSb, AlSb or InSb. After growth of 1.0 ML of GaSb on GaAs(0 0 1)-$c(4\times4)$ at 490°C, RHEED exhibited primary and half-order streaks along with weak transmission spots in the [1 1 0] direction, and chevrons in the [$\bar{1}$ 1 0] direction [18, 19]. The resulting surface morphology, shown in Fig. 1a, consists of a disordered distribution of 2D islands. The islands are somewhat elongated, with $\leqslant$ 1 ML-deep gaps between them [20]. Note that quantum dots (QDs) have not yet formed at this coverage. After deposition of a total of 3.5 ML GaSb, strong RHEED transmission spots were visible in both the [1 1 0] and [$\bar{1}$ 1 0] directions, indicating 3D growth. The distance between the spots was clearly smaller than the distance between the diffraction streaks, implying that the QDs had formed with a larger in-plane lattice constant than the GaAs substrate. Because ex situ TEM images of QDs on similarly prepared samples do not exhibit Moiré fringes [21], however, this change in lattice constant must not result from the formation of dislocations but rather must arise from the elastic relaxation of the GaSb bonds within the QD. The presence of QDs has been confirmed on similar samples by ex situ AFM, with typical densities of $1\times10^9/cm^2$, heights of 80 Å, and apparent diameters of 400 Å [21]. An STM image of a typical area between QDs is shown in Fig. 1b. (We try to avoid imaging QDs during studies of the wetting layer in order to avoid damage to the STM tip.) At this GaSb coverage, the wetting layer structure exhibits highly anisotropic ribbon-like structures oriented along the [$\bar{1}$ 1 0] direction. The characteristic ribbon separation, computed from the autocorrelation function for this image, is 50 Å in the [1 1 0] direction.

Ribbon-like wetting layers also result from the growth of AlSb on GaAs. We examined 2.0 ML of AlSb deposited on a (2×4) reconstructed GaAs surface at 500°C. After AlSb growth, the RHEED pattern revealed transmission spots superimposed on a (1×3) streak pattern. The resulting surface, shown in Fig. 2, is qualitatively similar to that following the growth of 3.5 ML of GaSb (Fig. 1b), with ribbon-like structures running along the [$\bar{1}$ 1 0] direction. The autocorrelation function yields a characteristic separation of 40 Å. Although not shown in this image, QDs are also present on the surface. Raman spectroscopy measurements of AlSb QDs on GaAs showed a two-mode

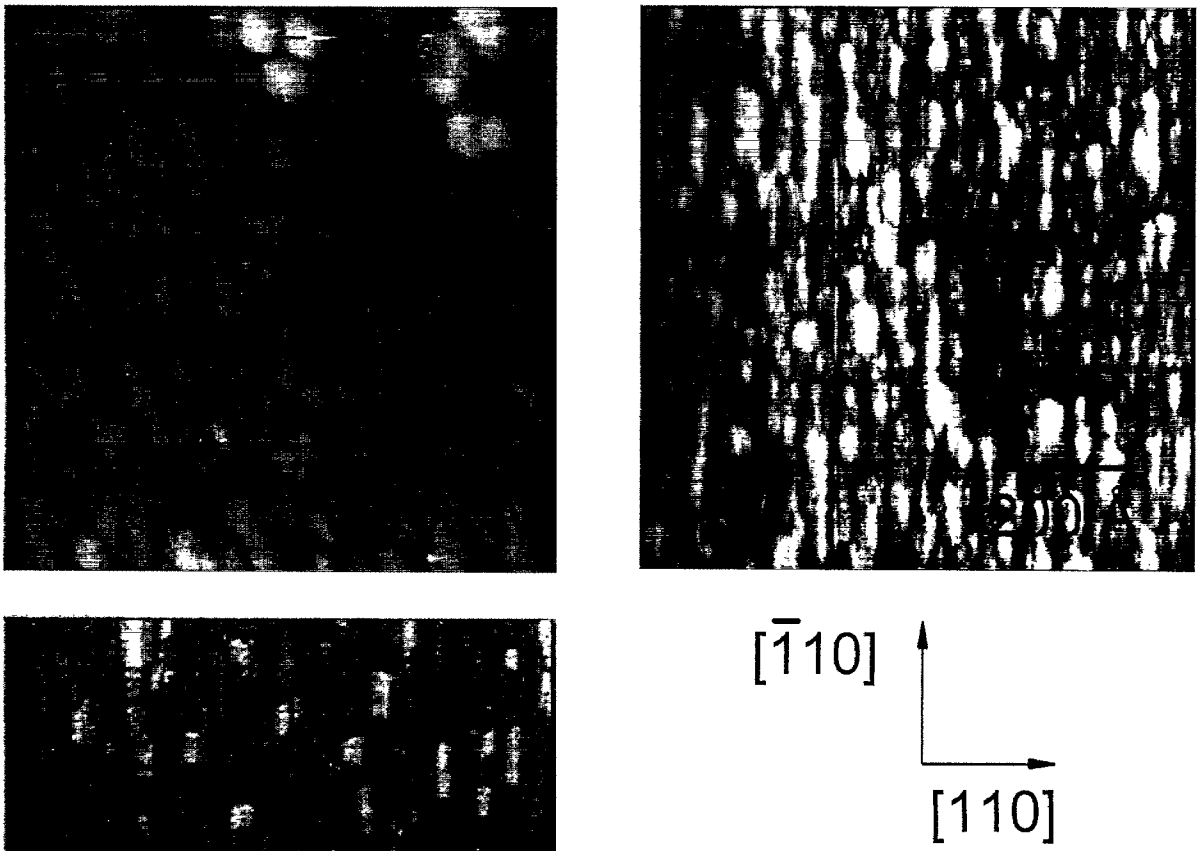

Fig. 2. Filled-state STM image of 2.0 ML of AlSb on GaAs(001)-(2 × 4). The gray-scale height range is approximately 12 Å.

behavior indicating the formation of an AlGaSb alloy due to Ga segregation [22]. Hence, the surface shown in Fig. 2 is more appropriately described as $Al_xGa_{1-x}Sb$.

Using ex situ AFM, we previously observed QDs after as little as 1.5 ML of InSb on GaAs [6]. In this study, we examined 1.5 and 2.0 ML of InSb on GaAs(0 0 1)-c(4 × 4) and 1.5 ML of InSb on GaAs(0 0 1)-(2 × 4) with STM. The substrate temperature during InSb growth was 410 C. In all three cases, RHEED revealed weak transmission spots in

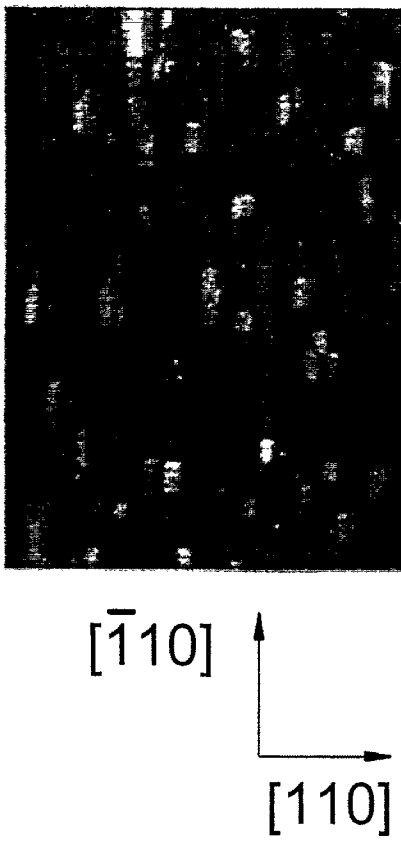

Fig. 1. Filled-state STM images of GaSb on GaAs(001)-c(4 × 4). GaSb coverages are: (a) 1.0 ML and (b) 3.5 ML. The gray-scale height ranges are approximately (a) 8 Å and (b) 10 Å. Quantum dots (not shown) are present on sample (b) but not on (a).

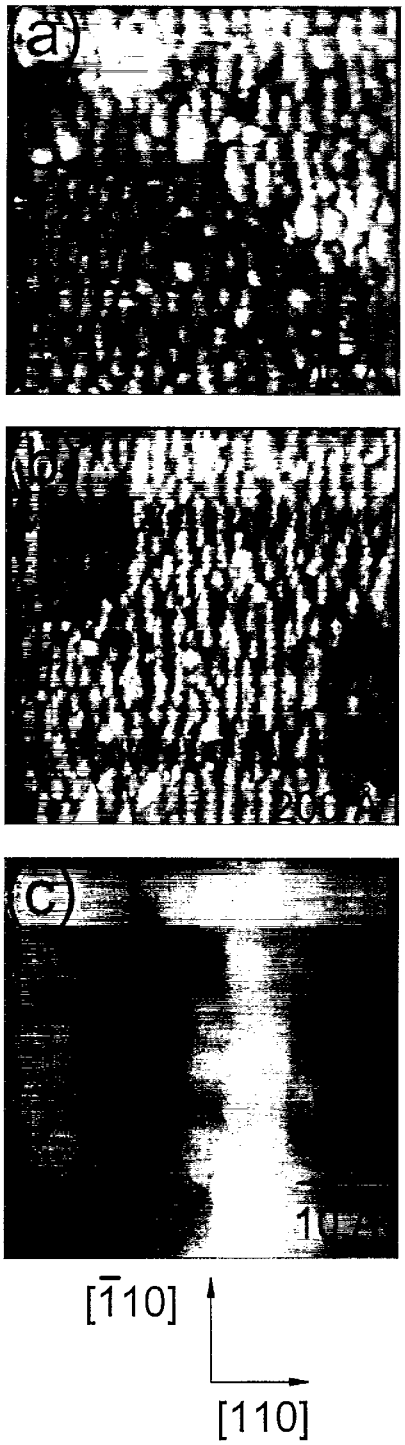

the [1 1 0] direction and chevrons in the [$\bar{1}$ 1 0] direction; STM and AFM confirmed the presence of QDs. In addition to coherent QDs, large dislocated islands were observed for each sample [23]. In Fig. 3a and Fig. 3b we show the STM images acquired between the QDs for 1.5 ML of InSb on GaAs-c(4 × 4) and GaAs-(2 × 4), respectively. Anisotropic ribbon-like structures are present for both initial substrate reconstructions. The characteristic ribbon separations from autocorrelation analyses are 50 Å for growth on GaAs-c(4 × 4) and 40 Å for growth on GaAs-(2 × 4). The characteristic length of the islands in the [$\bar{1}$ 1 0] direction is somewhat shorter for InSb deposition on the GaAs-c(4 × 4) reconstruction. Fig. 3c displays a higher magnification image of 1.5 ML of InSb on GaAs-(2 × 4), revealing atomic-scale structure. The surface appears to have a multilayer structure terminated by dimers (most likely Sb dimers).

4. Discussion

The traditional view of SK growth is that the initial deposition occurs as a continuous wetting layer. Our results, however, suggest a more complicated structure with a discontinuous morphology which may arise from a combination of effects. Both the relative surface energies of the absorbates and substrate, and the mismatch-related strain which may be relieved by the formation of vacancy lines, may play a role. A simple calculation, assuming complete strain relaxation by vacancy arrays, gives a spacing of 12.5 atomic planes or 54 Å for an 8% mismatch (GaSb or AlSb) and 6.8 atomic planes or 31 Å for InSb. These values are comparable to the characteristic separations of the ribbon-like structures found for all three materials.

A few groups have investigated the initial stages of InAs growth on GaAs by in situ STM.

Fig. 3. Filled-state STM images of 1.5 ML of InSb on GaAs: (a) GaAs(0 0 1)-c(4 × 4) starting surface, (b) GaAs(0 0 1)-(2 × 4) starting surface, and (c) higher magnification image of surface in (b). The gray-scale height ranges are approximately (a) 12 Å, (b) 12 Å, and (c) 8 Å. Note the monolayer-height (3 Å) steps visible in (a) and (b).

Bressler-Hill et al. examined submonolayer coverages of InAs grown on GaAs(0 0 1)-(2 × 4) surfaces [12]. They observed 2D InAs islands elongated along the [$\bar{1}$ 1 0] direction – the same direction found in this work. Based upon an examination of the scaling properties of the island size, they concluded that growth along the [$\bar{1}$ 1 0] direction behaves as if it is unstrained while growth in the [1 1 0] direction is quenched by strain. In contrast, Cirlin et al. studied InAs growth on GaAs(0 0 1)-c(4 × 4) and found wire-like structures oriented along the [1 0 0] direction (i.e. 45° from [$\bar{1}$ 1 0]) [15]. Because of the different symmetries of the (2 × 4) and c(4 × 4) reconstructions it is not surprising that for low coverages the features of the wetting layer would be oriented in different directions. We observe some evidence of this behavior in our data. Surfaces with 1.0 ML of GaSb (Fig. 1a) and 1.5 ML of InSb (Fig. 3a) on GaAs-c(4 × 4) are more isotropic than 1.5 ML of InSb (Fig. 3b) and 2.0 ML of AlSb (Fig. 2) on GaAs-(2 × 4), consistent with the more isotropic structure of the c(4 × 4) reconstruction. As indicated in Fig. 1b, however, after additional GaSb is deposited (3.5 ML total), the remnant character of the symmetry of the GaAs-c(4 × 4) surface reconstruction is eliminated and the wetting layer becomes highly anisotropic. The anisotropy of this structure does not appear to arise from kinetic limitations but, rather, is attributed to the direction-dependent strain associated with the dimer-based surface reconstructions of the wetting layers.

In addition to the impact of the reconstruction symmetry on the morphology of the wetting layer, the differences in the amount of As on the surface are also expected to influence the formation of antimonide quantum dots. For example, because the As coverage on a c(4 × 4) reconstruction is 1.75 ML [24], compared to 0.5 ML for a (2 × 4) surface [25], we expect the initial formation of AlAs (GaAs) when Al (Ga) is incident on a GaAs-c(4 × 4) surface. Because this material would not be under strain, the coverage required to form quantum dots could be expected to be larger for the GaSb and AlSb dots grown on the c(4 × 4) reconstruction. This is in agreement with our earlier studies of AlSb QD formation on the c(4 × 4) reconstruction which found that QDs did not form until over 3 ML AlSb had been deposited [6, 22]. This should be contrasted with the current study which shows that QDs form after only 2 ML of AlSb is deposited on the (2 × 4) reconstruction. This issue becomes even more complex for the deposition of InSb QDs on the c(4 × 4) reconstruction, where the initial deposition of In would be expected to form InAs. (The InSb/GaAs mismatch is twice as large as the InAs/GaAs mismatch.) AFM measurements on the samples of Fig. 3 revealed a higher density of both QDs and dislocated islands for the (2 × 4) reconstruction compared to the c(4 × 4) reconstruction.

5. Summary

Epilayers of GaSb, AlSb and InSb, with mismatches of 8–15%, exhibit a Stranski–Krastanov growth mode on GaAs(0 0 1). In situ STM measurements reveal that the wetting layers are not uniform, but consist of anisotropic, ribbon-like structures oriented along the [$\bar{1}$ 1 0] direction, with characteristic separations of 40–50 Å and heights of a few angstroms. These wetting layers coexist with self-assembled quantum dots. The initial GaAs surface reconstruction affects both the wetting layer structure and the QD density.

Acknowledgements

This work was supported by the Office of Naval Research.

References

[1] I.N. Stranski and L. Krastanov, Sitzungsber. Akad. Wiss. Wien. Math.-Naturwiss. K1 IIb 146 (1938) 797.
[2] E. Bauer, Z. Krist. 110 (1958) 372.
[3] R.W. Vook, Opt. Eng. 23 (1984) 343.
[4] P.M. Petroff and S.P. DenBaars, Superlattice Microstruct. 15 (1994) 15, and references therein.
[5] L. Samuelson, N. Carlsson, P. Castrillo, A. Gustafsson, D. Hessman, J. Lindalh, L. Montelius, A. Petersson, M.-E. Pistol and W. Seifert, Jpn. J. Appl. Phys. 34 (1995) 4392.
[6] B.R. Bennett, R. Magno and B.V. Shanabrook, Appl. Phys. Lett. 68 (1996) 505.
[7] E.R. Glaser, B.R. Bennett, B.V. Shanabrook and R. Magno, Appl. Phys. Lett. 68 (1996) 3614.

[8] F. Hatami, N.N. Ledentsov, M. Grundmann, J. Bohrer, F. Heinrichsdorff, M. Beer, D. Bimberg, S.S. Ruvimov, P. Werner, U. Gosele, J. Heydenreich, U. Richter, S.V. Ivanov, B.Ya. Meltser, P.S. Kopev and Zh.I. Alferov, Appl. Phys. Lett. 67 (1995) 656.
[9] C. Priester and M. Lannoo, Phys. Rev. Lett. 75 (1995) 93.
[10] C. Ratsch and A. Zangwill, Surf. Sci. 293 (1993) 123.
[11] C. Ratsch, P. Smilauer, D.D. Vvedensky and A. Zangwill, J. Phys. I France 6 (1996) 575.
[12] V. Bressler-Hill, S. Varma, A. Lorke, B.Z. Nosho, P.M. Petroff and W.H. Weinberg, Phys. Rev. Lett. 74 (1995) 3209.
[13] N.P. Kobayashi, T.R. Ramachandran, P. Chen and A. Madhukar, Appl. Phys. Lett. 68 (1996) 3299.
[14] Q. Xie, N.P. Kobayashi, T.R. Ramachandran, A. Kalburge, P. Chen and A. Madhukar, Mater. Res. Soc. Proc. 379 (1995) 177.
[15] G.E. Cirlin, G.M. Guryanov, A.O. Golubok, S.Ya. Tipissev, N.N. Lenentsov, P.S. Kopev, M. Grundmann and D. Bimberg, Appl. Phys. Lett. 67 (1995) 97.
[16] B.V. Shanabrook, J.R. Waterman, J.L. Davis and R.J. Wagner, Appl. Phys. Lett. 61 (1992) 2338.
[17] P.M. Thibado, E. Kneedler, B.T. Jonker, B.R. Bennett, B.V. Shanabrook and L.J. Whitman, Phys. Rev. B 53 (1996) R10481.
[18] Y. Nabetani, T. Ishikawa, S. Noda and A. Sasaki, J. Appl. Phys. 76 (1994) 347.
[19] R.P. Mirin, J.P. Ibbetson, K. Nishi, A.C. Gossard and J.E. Bowers, Appl. Phys. Lett. 67 (1995) 3795.
[20] P.M. Thibado, B.R. Bennett, M.E. Twigg, B.V. Shanabrook and L.J. Whitman, J. Vac. Sci. Technol. A 14 (1996) 885.
[21] B.R. Bennett, P.M. Thibado, M.E. Twigg, E.R. Glaser, R. Magno, B.V. Shanabrook and L.J. Whitman, J. Vac. Sci. Technol. B 14 (1996) 2195.
[22] B.R. Bennett, B.V. Shanabrook and R. Magno, Appl. Phys. Lett. 68 (1996) 958.
[23] B.R. Bennett, B.V. Shanabrook, E.R. Glaser, R. Magno and M.E. Twigg, Superlattice Microstruct. 21 (1997).
[24] D.K. Biegelsen, R.D. Bringans, J.E. Northrup and L.-E. Swartz, Phys. Rev. B 41 (1990) 5701.
[25] J. Zhou, Q. Xue, H. Chaya, T. Hashizume and T. Sakurai, Appl. Phys. Lett. 64 (1994) 583.